On the Rate of Frazil Ice Formation in Polar Regions in the Presence of Turbulence

S. I. VOROPAYEV,* H. J. S. FERNANDO, AND L. A. MITCHELL

Department of Mechanical and Aerospace Engineering, Environmental Fluid Dynamics Program, Arizona State University, Tempe, Arizona

(Manuscript received 28 July 1994, in final form 28 October 1994)

ABSTRACT

The purpose of this paper is to present the results of a series of laboratory experiments aimed at understanding the frazil ice growth in polar regions during the summer whence a freshwater layer at temperature 0°C spreads between an old ice sheet and underlying salty seawater that is at its freezing point. The aim of the experiments was to study the influence of external turbulence on the rate of new frazil ice formation. The experiments were conducted in a large walk-in freezer at a temperature near 0°C. To produce controlled turbulence, two oscillating grids were installed in a tank filled with two layers of water: fresh water at temperature 0°C in the upper layer and salty (35 psu) cold water at temperature −1.9°C in the bottom layer. During the experiments, the bottom layer was cooled from below, using Peltie elements, and its temperature was near the freezing point. The turbulence induced in both layers facilitates the transport of heat across the density interface between layers, and as the time progresses the lower boundary of the upper layer becomes overcooled, and small crystals of frazil ice intensively form in this overcooled zone. These buoyant crystals rise to the surface, and with time a sheet of frazil ice is formed at the surface of the fresh water. It is found that the rate of frazil ice formation in the presence of turbulence is a function of the interfacial Richardson number and is much higher (30–100 times) than the case where there is no turbulence. A theoretical explanation is given to explain these observed high ice formation rates.

1. Introduction

During the summers of Arctic and Antarctic Oceans, the solar heating melts the upper surface of the ice sheet and the fresh meltwater spreads over the ice coves. A bulk of this water flows on the ice and then drains through the cracks and other openings into the ocean. Now, the fresh meltwater spreads under the ice cover over cold, salty (23–35 psu) seawater forming a two-layer stratification, as shown schematically in Fig. 1. Both water layers are at their freezing points: the upper layer is at 0°C and the bottom layer is at −1.6 to −1.9°C. The thick ice sheet isolates the ocean from the atmosphere, and the heat exchange between the two is negligibly small. As was pointed out a century ago by Nansen (1897), the cooling from below is the only possible source of ice creation during polar summers. The later observations (Zubov 1963; Hanson 1965; Kozlovskii 1971; Cherepanov and Kozlovskii 1962) confirmed Nansen's conclusion and estimated the thickness of the newly formed ice sheet as of the order 1 m and more. A similar process takes place in fjords and river gulfs when cold river water flows over a brackish seawater layer of near freezing temperature.

Since the rate of heat transfer across the temperature–salinity interface between the two layers is much larger than the rate of salt transport (Fig. 1), the lower part of the upper fresh water becomes overcooled, and frazil ice is formed. The term "frazil ice" is usually used for small discs of ice that form in turbulent slightly supercooled water (Martin 1981). Once frazil ice crystals are formed, they rapidly aggregate together and stick on to foreign material and the overlying ice sheet. This leads to new ice and to the increase of the thickness of the primary ice cover.

Although the basic mechanism here appears to be rather simple, many details are still unclear, and the processes involved were reproduced using laboratory experiments only recently. These studies were concentrated on the case where the motion is slow and is induced by convective instabilities of the upper layer (Martin and Kauffman 1974) or of both layers (Stigebrandt 1981). The estimates, as obtained in the laboratory experiments, for the rate of ice formation for these cases give value of order 1–2 mm per day; this seems realistic for some specific places where the motions are dynamically isolated from the background turbulent motions, but certainly these estimates are

* Additional affiliation: Institute of Oceanology, Russian Academy of Sciences, Moscow, Russia.

Corresponding author address: Prof. Harindra J. Fernando, Department of Mechanical and Aerospace Engineering, College of Engineering and Applied Sciences, Arizona State University, Tempe, AZ 85287-6106.
E-mail: j.fernando@asu.edu

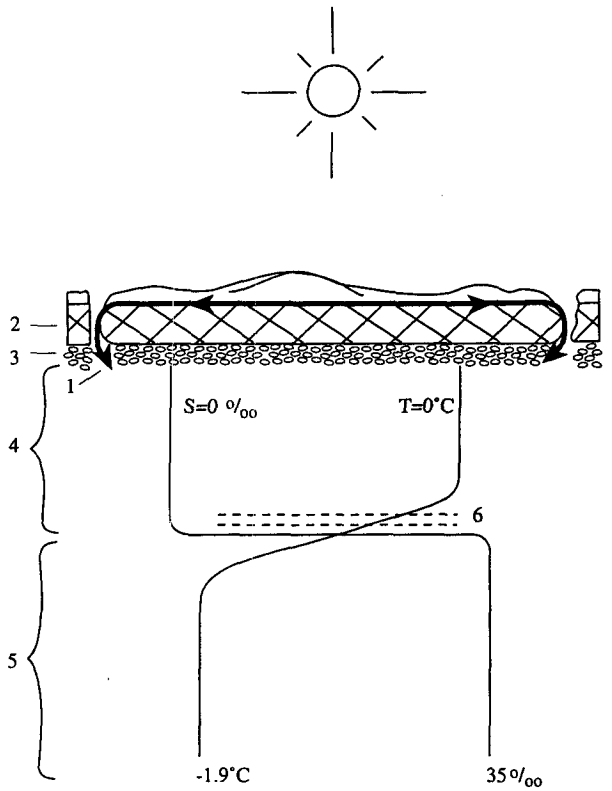

FIG. 1. A schematic of frazil ice formation in polar regions during the summer: 1) fresh melt water from solar heating; 2) old ice sheet; 3) new frazil ice sheet; 4) fresh water at 0°C; 5) salty ocean water at −1.9°C (35 psu); and 6) supercooled water.

too small to explain the observed thicknesses of newly formed frazil ice sheets, which are typically 1 m or more.

Taking into account that weak convective motions lead to an increase of the heat transfer by a factor of 5–10 compared to classic heat diffusion theory (Martin and Kauffman 1974), it is clear that more intense turbulent motion may significantly increase this ratio.

Combined heat–salt turbulent transports across a density interface have been studied using laboratory experiments by Voropayev et al. (1988) and Krylov and Zatsepin (1992). Based on the results of these experiments, which were conducted at room temperature, a theoretical model for the frazil ice formation was also proposed in Krylov and Zatsepin (1992). This model predicts a significant increase in the rate of frazil ice formation, up to 10 cm per day, and in the presence of intensive turbulence the predicted values are much higher.

So far, no experiments have been performed to study the formation of frazil ice under conditions that are closer to natural conditions at higher latitudes, and hence no data exist to verify the estimates of various models. The main purpose of the present study is to undertake this task and to shed light on the mechanics of frazil ice formation in two-layer systems, in which the fluid layers are at near freezing points and are turbulent with both heat and salt stratifications contributing to the density jump at the interface.

2. Experimental installation and method

The experiments were conducted in a large (200 × 200 × 200 cm) walk-in freezer. During the experiments the temperature in the box was fixed and was maintained near 0 ± 1°C. The frazil ice formation was studied in a tank of square cross section 37 × 37 cm and 50 cm deep. The side walls of the tank were made from Plexiglas and the bottom consisted of an aluminum plate. Two horizontal grids made of Plexiglas rods of square cross section (1 × 1 cm) and a mesh size 4.5 cm were installed in the tank (Fig. 2) and the upper grid was fixed to the lower one via three steel rods of small diameter (0.3 cm). The rods were covered with plastic paint to reduce ice formation. The distance between grids was 25 cm, and the lower grid was located at a distance 5 cm from the bottom of the tank. The lower grid was fixed to a vertical oscillating rod that was connected through the tank bottom to an eccentric template driven by a d.c. motor. The grid assembly

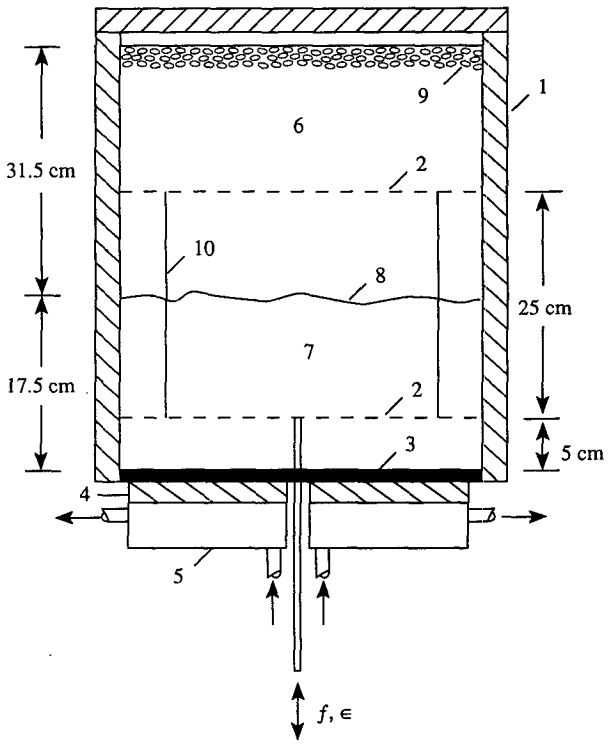

FIG. 2. A sketch of the experimental apparatus: 1) tank with insulation; 2) grids oscillating in the vertical direction with a frequency f and stroke ϵ; 3) aluminum bottom; 4) Peltie elements; 5) cooling system with water for Peltie elements; 6) fresh water at 0°C; 7) salt water (35 psu) at −1.9°C; 8) density interface; 9) sheet of frazil ice; and 10) steel rods connecting the grids.

was oscillated in the vertical direction with adjustable frequency (f = 0–4 Hz) and stroke (ϵ = 1–3.5 cm). Precautions were taken to prevent vibration of the grid in the horizontal plane.

To cool the tank from below, five ceramic Peltie elements were installed at the air side of the aluminum bottom. Cold surfaces of the elements were in contact with the bottom of the tank, and the heat transfer was facilitated by applying thermogrease between the surfaces. To obtain the maximum cooling rate, the outer hot surfaces of the Peltie elements were cooled by cold water at 1.0 ± 0.5°C, which was continuously circulated through the aluminum boxes fixed to the outer hot surfaces of the elements (Fig. 2). By changing the voltage applied, it was possible to change the heat flux q through the bottom of the tank (q = 0 to 0.83 kJ m^{-2} s^{-1}).

To reduce heat exchange through the side surfaces, sheets of styrofoam insulation were attached to the sides of the tank. A standard method was used to estimate the rate of heat exchange through the surfaces of the tank. In this method, the tank was filled with water at temperature T_0, which is higher than the mean temperature $T_a \approx 20$°C of the room. The upper surface of the tank was covered with a sheet of Plexiglass, above which a layer of insulation was placed. The water in the tank was mixed periodically by oscillating the grids, and the mean temperature T of water in the tank was measured as a function of time. The results of the measurement of the nondimensional temperature excess $\theta = (T - T_a)/(T_0 - T_a)$ as a function of time t were plotted, and the results are shown in the log–linear plot of Fig. 3. The solid line through the data points represents the function

$$\theta = \frac{T - T_a}{T_0 - T_a} = \exp(-t/\tau), \qquad (1)$$

with τ = 2400 min. The heat balance for water in the tank is

$$\rho c_p V \frac{dT}{dt} = -q_0 B, \qquad (2)$$

where $T(t)$ is a mean temperature given in (1); ρ and c_p are the density and specific heat capacity of water, respectively; $V = HD^2$; H and D are the depth of water and the width of the tank, respectively; and $B = 2D(2H + D)$ is the total surface of the tank. Using (2), we obtain the estimate for the mean heat flux q_0 through the water surfaces of the tank

$$q_0 \approx -(T - T_a)\rho C_p \frac{HD}{2(2H + D)\tau}. \qquad (3)$$

During the experiments, the temperature in the freezing box was maintained at $T_a = 0 \pm 1$°C, and the temperature in the upper layer was near 0°C. This gives the estimate $q_0 \approx \pm 2.1 \times 10^{-3}$ kJ m^{-2} s^{-1}. That is, negligibly small compared to the typical values of the heat flux q through the bottom of the tank.

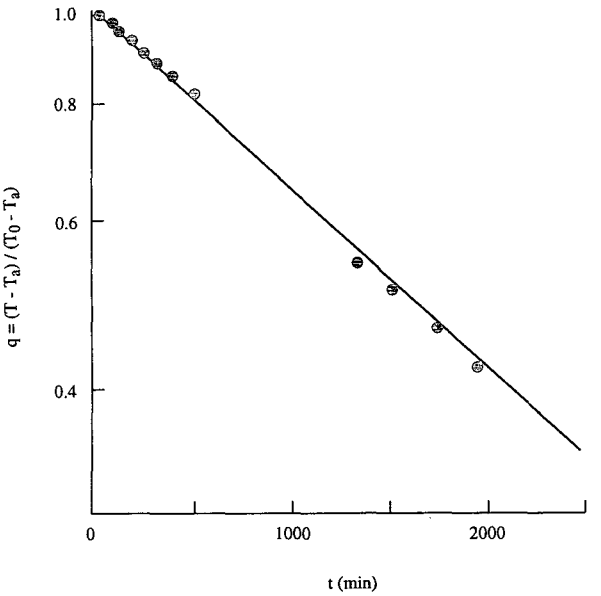

FIG. 3. Nondimensional excessive temperature in the tank $\theta = (T - T_a)/(T_0 - T_a)$ as a function of time t. A semilog plot is shown; dots show measured values and solid line shows function (1) with τ = 2400 min.

The initial conditions of the experiments were set up as follows. The tank was filled with two layers of water of depths H_1 = 31.5 cm and H_2 = 17.5 cm at 0°C. Thus, there was a gap of 1 cm between the free surface and the cover of the tank. The upper layer (H_1) was fresh water and the lower layer (H_2) was salt water with salinity at 35 psu. The initial temperature distribution was achieved by activating the cooling system at the bottom, and water in both layers was mixed periodically by slowly oscillating the grids. This was continued until the temperature T_2 of the salt water in the lower layer reached approximately its freezing point (−1.9°C). The initial distributions of salinity and temperature are shown schematically in Fig. 1.

The temperature T_1 of the upper layer was measured continuously with an accuracy of ±0.1°C by a standard digital thermometer operating with a platinum resistance sensor. To measure the temperature difference $\Delta T = T_2 - T_1$ between the layers, copper–constantan thermocouples were used. The time constant of the thermocouples was artificially increased (≈30 s) to obtain smooth temperature data at the middle of the layers. Voltage from the thermocouples was passed through a low-noise amplifier and was recorded continuously on a X–Y plotter. This permitted the control of the temperature difference ΔT between the two layers with an accuracy of ± 0.05°C. When the desired initial distribution of temperature was reached, the grids were activated and the experiments with frazil ice formation was begun.

During the experiments, the salinity S_2 of the lower layer decreases with time. The salinities S_1 and S_2 of both layers were determined by measuring the refractive index of a small amount of fluid sampled periodically from the middle of both layers by withdrawing fluid with a syringe fitted with a long needle.

To realize the freezing point conditions

$$T_i + aS_i = 0 \quad (i = 1, 2) \tag{4}$$

[$a = 0.056°C\ (psu)^{-1}$, see e.g., Lide (1993)], that is, both layers are at their own freezing temperatures, the following procedure was adopted. Using the measured value of $\Delta S = S_2 - S_1$, the required temperature difference $\Delta T = T_2 - T_1$ between the two layers was estimated using (4) and the cooling rate q was periodically adjusted by changing the voltage applied to the cooling elements so that the measured value of ΔT was in accordance with the estimate.

The optimal distance (25 cm) between the grids was chosen due to the following reason. Due to the cooling of the bottom, a layer of cold salt water is formed near the bottom of the tank. At salinities greater than about 25 psu, the density of salt water at temperatures near its freezing point increases with decreasing temperature. To mix this dense water over the entire lower layer, a certain amount of turbulent kinetic energy is required.

For a given frequency f, stroke ϵ of oscillation, and a stabilizing buoyancy flux q, the maximum depth H_*, where a fluid can be mixed by turbulence, is given by (Kantha and Long 1980; Benilov et al. 1993)

$$\frac{H_*}{\epsilon} = c\left(\frac{\epsilon^2 f^3 c_p \rho}{\alpha g q}\right)^n, \tag{5}$$

where g is the gravity acceleration, α is the thermal coefficient of water expansion, and c and n are empirical constants that depend on the geometry of the grid. For the grids used in the present experiments, $c = 1.1$, $n = 0.25$ (Benilov et al. 1993). Thus, the distance between the lower grid and the density interface, which is equal to the half of the distance between the grids (see Fig. 2), must not exceed H_* given by (5). For typical values of the present experiments, (5) gives the estimate $H_* \geqslant 14$ cm; the half distance between the grids was 12.5 cm, and hence this requirement was satisfied.

The distance between the lower grid and the bottom of the tank was chosen empirically. In a preliminary run, when this distance was equal to 12 cm, the ice was formed at the aluminum bottom during the run. To reduce the ice formation here, the intensity of turbulence near the bottom was increased by decreasing the distance between the lower grid and the bottom to 5 cm.

The characteristics of turbulence induced by oscillating grids have been well studied as functions of external parameters such as the frequency f, the stroke ϵ of oscillation, and the mesh size M of grid (see e.g., Thompson and Turner 1975; Hopfinger and Toly 1976). Accordingly, the typical velocity (rms) and (integral) length scale of turbulence u and l induced by the oscillating grids at the distance z from the grid is given by

$$u = c_1 M^{1/2} f \epsilon^{3/2} z^{-1}, \qquad l = c_2 z, \tag{6}$$

where for the present grids $c_1 = 0.3$ and $c_2 = 0.1$ can be estimated following the procedure used by E and Hopfinger (1986); thus, near the interface $z = 12$ cm. The nature of the density interface, for this kind of experiments, is usually characterized by the interfacial Richardson number, defined by

$$\mathrm{Ri} = g\frac{\Delta\rho l}{\rho u^2}, \tag{7}$$

where $\Delta\rho = \rho_2 - \rho_1$ is the density jump between two layers and ρ is the mean density of the fluid. In general, $\Delta\rho = \rho(\beta\Delta S - \alpha\Delta T)$, where ΔS and ΔT are salinity and temperature jumps, respectively, across the density interface. In our experiments $\alpha\Delta T$ is small compared to $\beta\Delta S$ ($\beta \approx 8 \times 10^{-4}\ (psu)^{-1}$ and $\alpha \approx 2 \times 10^{-5}\ °C^{-1}$, see Lide 1993), hence with good accuracy, $\Delta\rho \approx \rho\beta\Delta S$.

3. Results of observations

After the initial conditions shown in Fig. 1 were reached, the grids were activated and oscillated with a fixed frequency. To initiate the ice formation in the system, a small amount of ice crystals was imposed into the fluid, using the following procedure. The bottom cooling rate was adjusted to its maximum within 2–5 min and then was returned to the desired level. This leads to the formation of small ice crystals at the bottom. Then the cooling water for the hot surfaces of the Peltie elements was stopped for a short time, thus forcing the Peltier elements to act as heating elements. The resulting slight bottom heating caused some of the ice crystals to melt, detach from the bottom, and then disperse throughout the fluid. Without artificial seeding of ice crystals into the system, the mean temperature of fresh water in the upper layer decreases with time below the freezing point, but no ice is formed in such a system.

Following the above procedure, intense formation of ice crystals in a system was clearly visible. With time the ice crystals were found to rise to the surface, forming a sheet of frazil ice. A typical ice sheet, which was formed at the end of an experiment, is shown in the photograph of Fig. 4. Here, only the central part of the experimental tank is illuminated by an intense light sheet from the top, and only the central part of the ice sheet is clearly visible. This photograph was taken at an angle oblique to the horizontal, thus enabling clear visibility of the ice sheet.

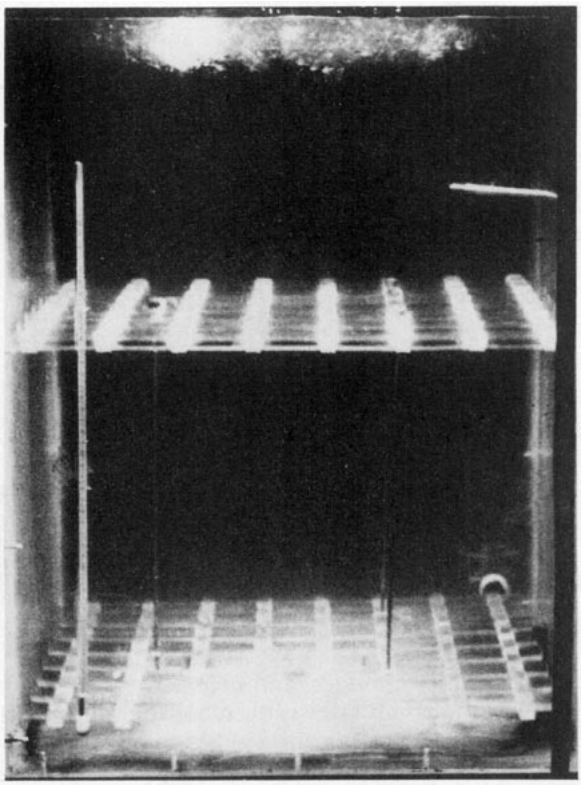

FIG. 4. Side-view photograph of the experiment. The illumination is provided by a diverging light beam emanating from an arc lamp directed at the ice sheet. The ice sheet formed at the surface of the upper-water layer is clearly seen. The experimental parameters are initial Richardson number $Ri_0 = 106$; time from beginning of the experiment $t = 126$ min; and the depths of the ice sheet $h = 2.6$ cm.

The details of the frazil ice formation process is described below. The visual observations revealed that, after the artificial seeding of ice crystals into the system, the ice is mostly formed in a relatively narrow zone (1–2 cm in depth) in the vicinity of the upper part of the density interface, between the two layers, where the water is overcooled and provides favorable conditions for ice formation (Fig. 1). Because the temperature interface is usually thicker than the salinity interface [(see e.g., Fig. 3 of Krylov and Zatsepin (1992)], the fresh water at the bottom of the upper layer is at subzero temperatures, and ice crystals are intensely formed here. Under these conditions, the temperature at the middle of the upper layer was slightly above 0°C (0.05° to 0.1°C).

The buoyant ice crystals formed in the overcooled zone were found to melt during their ascent to the surface, thus cooling the surrounding fluid. As a result, after about 3–5 min, the temperature in the upper layer dropped slightly below 0°C. Consequently, the distribution of rising ice crystals became approximately homogeneous in the whole depth of the upper layer. Small buoyant ice crystals, formed in the overcooled zone, rose to the surface with a typical velocity of the order of several millimeters per second. At the surface some crystals fused to each other forming platelets, which agglomerate in somewhat ordered clusters to form ice floes; within 5–10 min, a thin (0.05–0.1 cm) ice cover appeared at the surface. This cover had numerous holes between the ice floes and approximately 2/3 of the surface of water was covered by ice, another 1/3 of the surface being open water. The upper side of this thin cover was relatively smooth, with most of the floes oriented horizontally; the lower surface was rather irregular with some crystals oriented in the vertical plane.

The ice crystals arriving at the surface were trapped by the ice cover, and with time, the thickness of the ice sheet was measured (Fig. 5). The lower boundary of this sheet is irregular (Fig. 6), and new ice crystals, arriving from the depth, formed large clusters with a typical size of order 0.5–1.0 cm. These clusters are not

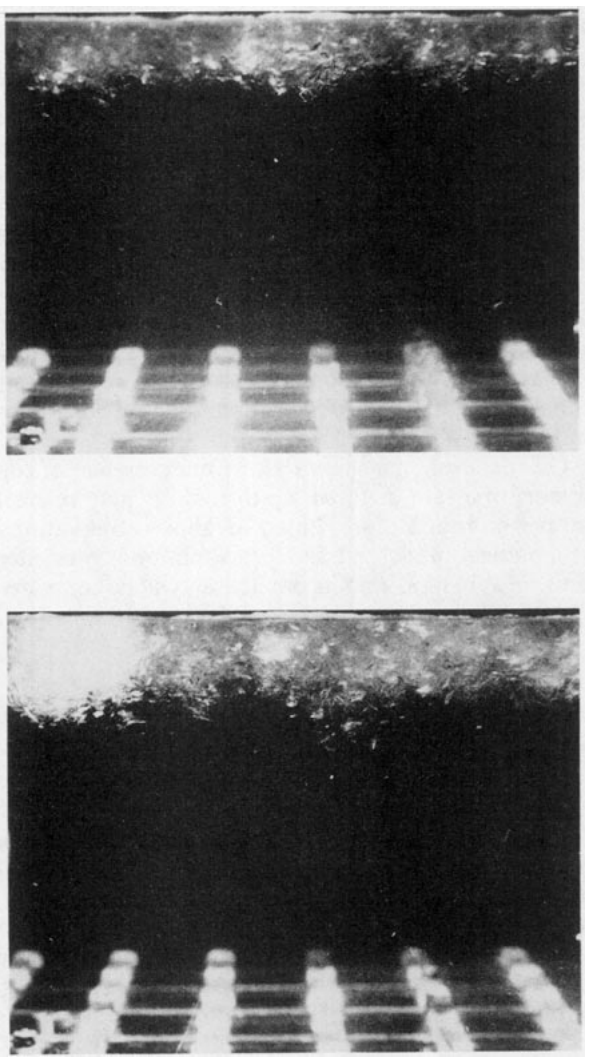

FIG. 5. A sequence of photographs, showing the growth of the frazil ice sheet with time in an experiment with $Ri_0 = 106$; (upper) $t = 48$ min, $h = 1.4$ cm and (lower) $t = 93$ min, $h = 2.5$ cm.

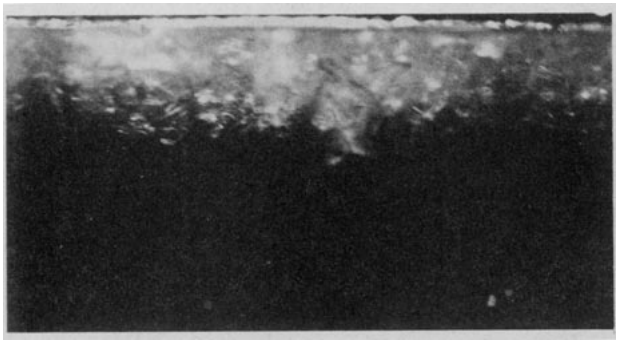

FIG. 6. Typical structure of the lower boundary of the frazil ice sheet at the water surface of the experiment with $Ri_0 = 106$.

FIG. 7. A large cluster of ice crystals, which is fused to the metal support of the thermocouples at the level of the overcooled zone, 1–2 cm up from the middle of the density interface. The density interface is partly visible as a wavy shadow below the cluster. The scale is marked to the right, with distance between the marks indicating 1 cm.

evident in Fig. 6 (which presents only an average oblique view) but are shown in Fig. 7. This particular ice cluster is fused to the metal support of the thermocouples at the level of the overcooled zone at the bottom of the upper layer.

Similar (but smaller) ice clusters with chaotically oriented crystals cling to each other and form the irregular lower boundary of the ice sheet. Some of the water from the upper layer appeared to be trapped between the large ice clusters. In fact, the resulting ice sheet is a mixture of ice conglomerates of volume fraction I_0, with the rest $(1 - I_0)$ being the water. To determine I_0, the ice sheet was collected using a fine copper net at the end of each experiment. Collected ice was then weighed and the mean value of I_0 was determined. This gave an estimate of $I_0 = 0.25 \pm 0.03$, which is in agreement with the typical estimates $I_0 = 0.3$ obtained from the field observations (e.g., Cherepanov and Kozlovskii 1972).

Our experiments show that in the presence of turbulence the rate of frazil ice formation may reach 1 cm per hour and more. Based on above observations, a theoretical model of frazil ice formation is presented in the next section, and its predictions will be compared with the laboratory experimental measurements.

4. A model and some estimates

Krylov and Zatsepin (1992) considered a simple model of frazil ice formation in the presence of turbulence. This model dealt with steady processes, and herein the more general unsteady case will be analyzed. The system under consideration is shown schematically in Fig. 8. The upper layer of depth H_1 and the lower layer of depth H_2 contain water of salinity, temperature, and density $S_{1,2}$, $T_{1,2}$, and $\rho_{1,2}$, respectively, and $\Delta S = S_2 - S_1 > 0$, $\Delta T = T_2 - T_1 > 0$. The contribution of ΔT for the density difference $\Delta\rho = \rho_2 - \rho_1$ is negligibly small; namely, $\Delta\rho = \rho\beta\Delta S$. The lower layer is cooled from below, so that the rate of cooling q is sufficient to maintain water in both layers near their freezing temperatures, determined by (4). The temperature interface between these two layers is broader than the salinity interface, and hence the water at the bottom of the upper layer is overcooled and frazil ice is formed. The ice that is formed has salinity S_0, temperature T_1, and density ρ_0. The distribution of ice crystals in the upper layer is uniform, with a volume concentration J_0. The ice sheet at the surface of the upper layer consists of a mixture of ice crystals (with volume concentration I_0, salinity S_0, temperature T_0, and density ρ_0) and water from the upper layer (salinity, temperature, and density S_w, T_0, and ρ_w, respectively); the thickness of the ice sheet is h.

Turbulence is induced in both layers by oscillating grids (or some other mechanism in natural conditions),

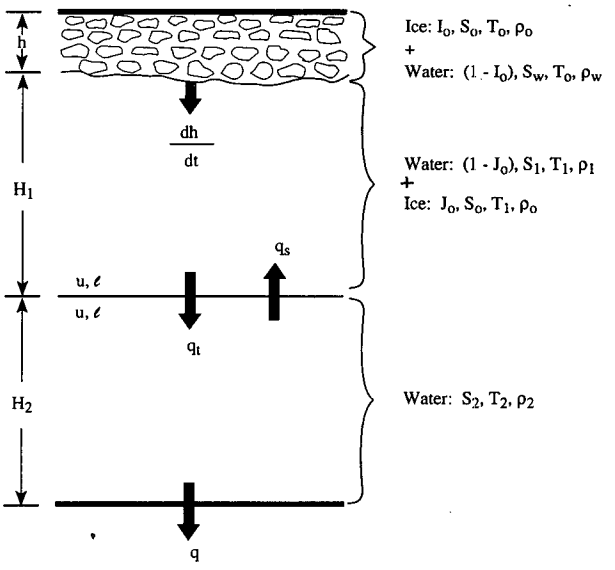

FIG. 8. A schematic of the model flow configuration.

and near the interface it is characterized by typical velocity and length scale of u and l that are determined by (6). The intensity of mixing across the density interface is assumed to be determined by the interfacial (local) Richardson number Ri, given by (7), and the induced turbulent fluxes of salt q_s and heat q_t across the interface are functions of Ri. These functions were determined experimentally by Voropayev et al. (1988) and Krylov and Zatsepin (1992) for a two-layer system for different values of $\Delta S > 0$ and $\Delta T < 0$. Accordingly, for small ΔT values q_t and q_s are given by

$$\frac{\left(\frac{q_t}{\rho c_p \Delta T}\right)}{u} = -c_t \,\mathrm{Ri}^{-1/2}, \tag{8}$$

$$\frac{\left(\frac{q_s}{\rho \Delta S}\right)}{u} = c_s \,\mathrm{Ri}^{-3/2}, \tag{9}$$

where c_t = constant = 8×10^{-2}, c_s = constant = 0.56 in the range $10 \leqslant \mathrm{Ri} \leqslant 10^3$, and c_p is the specific heat capacity of water.

Although the empirical relations (8) and (9) were obtained during the experiments with room temperature (20°C), it seems reasonable to assume that they are valid for low temperatures also because the temperature contribution to the density jump $\Delta\rho$ is negligible at small ΔT. Also note that the geometrical parameters for these experiments (e.g., tanks and grid sizes) were very similar to that of the present experiments.

To derive governing equations for the problem, consider the balances of mass, salinity, and heat in the lower layer (thickness: H_2) and in the upper layer with the ice sheet (thickness: $H_1 + h$). Using the notation of Fig. 8, the mass balance of salt water take the form

$$\frac{d}{dt}(H_2\rho_2) = 0, \tag{10}$$

$$\frac{d}{dt}\{H_1[(1 - J_0)\rho_1 + J_0\rho_0] + h[(1 - I_0)\rho_w + I_0\rho_0]\} = 0. \tag{11}$$

The balances of salt give

$$\frac{d}{dt}(H_2\rho_2 S_2) = -q_s, \tag{12}$$

$$\frac{d}{dt}\{H_1[(1 - J_0)\rho_1 S_1 + J_0\rho_0 S_0] + h[(1 - I_0)\rho_w S_w + I_0\rho_0 S_0]\} = q_s. \tag{13}$$

If the latent heat of freezing is λ and the heat capacity of ice layer is c_0 ($\lambda = 80$ cal gr^{-1}, $c_0 = 0.5\, c_p$, $\rho_0 = 0.916$ gr cm^{-3}, e.g., see Hobbs 1974), the heat balance for the layers may be presented in the form

$$\frac{d}{dt}(H_2 c_p \rho_2 T_2) = q_t - q, \tag{14}$$

$$\frac{d}{dt}\{H_1[(1 - J_0)c_p\rho_1 T_1 + J_0\rho_0(c_0 T_1 - \lambda)] + h[(1 - I_0)c_p\rho_w T_0 + I_0\rho_0(c_0 T_0 - \lambda)]\} = -q_t. \tag{15}$$

The set of equations (10)–(15) is too complicated for the analysis and can be simplified with a few assumptions to a reasonable degree of accuracy. They are: the salinity S_0 of pure ice is practically equal to zero, $S_0 = 0$; the differences in densities $\Delta\rho$ become important only when $\Delta\rho$ is multiplied by some large coefficient, for example when the product $\Delta\rho g$ is used, as in (7). Thus, let $\rho_1 \approx \rho_2 \approx \rho_w \approx \rho_0 = \rho = \text{const}$. It is also reasonably accurate to assume $J_0 \ll I_0$, $c_p T_{0,1,2} \ll \lambda$, $h \ll H_1$. Using these simplifications, (10)–(15) may be reduced as

$$\frac{dH_2}{dt} = 0, \tag{16}$$

$$\frac{d}{dt}(H_1 + h) = 0, \tag{17}$$

$$\rho H_2 \frac{dS_2}{dt} = -q_s, \tag{18}$$

$$\rho H_1 \frac{dS_1}{dt} = q_s + \rho[S_1 - (1 - I_0)S_w]\frac{dh}{dt}, \tag{19}$$

$$c_p \rho H_2 \frac{dT_2}{dt} = q_t - q, \tag{20}$$

$$c_p \rho H_1 \frac{dT_1}{dt} = \rho\lambda I_0 \frac{dh}{dt} - q_t. \tag{21}$$

Using (4), and after some algebra, (19) and (21) give the estimate for the rate dh/dt of frazil ice formation as

$$\frac{dh}{dt} = \frac{(q_t - ac_p q_s)}{\rho\{I_0\lambda + ac_p[S_1 - (1 - I_0)S_w]\}}. \tag{22}$$

Using for q_t and q_s the relations (8) and (9), by neglecting the small second term in the denominator of (22) and by taking into account (4), we obtain the expression for nondimensional rate of frazil ice formation

$$\frac{dh/dt}{u} = \Delta S_0 \left(\frac{\Delta S}{\Delta S_0}\right)^{1/2} \mathrm{Ri}_0^{-1/2} \frac{c_p a c_t}{\lambda I_0} \times \left[1 - \frac{c_s}{c_t}\mathrm{Ri}_0^{-1}\left(\frac{\Delta S}{\Delta S_0}\right)^{-1}\right]. \tag{23}$$

Here $\Delta S_0 = \Delta S\,(t = 0)$ is the initial salinity difference between the two layers and $\mathrm{Ri}_0 = \mathrm{Ri}(t = 0)$ is the initial Richardson number defined by

$$\mathrm{Ri}_0 = \frac{g\beta\Delta S_0 l}{u^2}. \tag{24}$$

The addition of (20) and (21), together with (18), (19), and (4) can be used to obtain the estimate

$$q = \rho\lambda I_0 \frac{dh}{dt}. \tag{25}$$

To estimate the dependence of $\Delta S/\Delta S_0$ on time t, one can use (18) and (19). Using (9) for q_s and by neglecting the small second term in (19), we obtain

$$\frac{d}{dt}\left(\frac{\Delta S}{\Delta S_0}\right) = -(H_1^{-1} + H_2^{-1})c_s u\,\mathrm{Ri}_0^{-3/2}\left(\frac{\Delta S}{\Delta S_0}\right)^{-1/2}. \tag{26}$$

Integrating (26) with the initial condition $\Delta S/\Delta S_0 = 1$ at $t = 0$, we get

$$\frac{\Delta S}{\Delta S_0} = \left[1 - \frac{3}{2}(H_1^{-1} + H_2^{-1})c_s u\,\mathrm{Ri}_0^{-3/2} t\right]^{2/3} = \left(1 - \frac{t}{\tau_0}\right)^{2/3}, \tag{27}$$

where the timescale

$$\tau_0 = \left[\frac{3}{2}(H_1^{-1} + H_2^{-1})c_s u\,\mathrm{Ri}_0^{-3/2}\right]^{-1} \tag{28}$$

is introduced for brevity. Note that for $t > t_0$, the two layers will be mixed, and the solutions are no longer valid. Substituting (27) into (23), we obtain the first-order differential equation for h

$$\frac{dh/dt}{u} = \frac{c_p a}{\lambda I_0}\Delta S_0 c_t\,\mathrm{Ri}_0^{-1/2}\left(1 - \frac{t}{\tau_0}\right)^{1/3} \times\left[1 - \frac{c_s}{c_t}\mathrm{Ri}_0^{-1}\left(1 - \frac{t}{\tau_0}\right)^{-2/3}\right]. \tag{29}$$

This equation can be easily integrated if we neglect the second term in square brackets; for example for $\mathrm{Ri}_0 \gg c_s/c_t \approx 7$. This gives the estimate

$$h = \frac{c_p a}{\lambda I_0}\Delta S_0 u c_t \tau_0\,\mathrm{Ri}_0^{-1/2}\left[1 - \left(1 - \frac{t}{\tau_0}\right)^{4/3}\right], \tag{30}$$

which is valid only for $\mathrm{Ri}_0 \gg 7$ and $t < \tau_0$. Now, the main characteristics of the fluid system under consideration can be estimated and comparisons with the measured values can be made.

In two experiments, which were conducted at $\mathrm{Ri}_0 = 422$ ($\Delta S_0 = 35$ psu, $f = 2$ Hz, $\epsilon = 2.0$ cm) and Ri $= 106$ ($\Delta S_0 = 35$ psu, $f = 4$ Hz, $\epsilon = 2.0$ cm), the depth h of the ice sheet as well as $S_{1,2}$ and $T_{1,2}$ were measured as functions of time. The mean lower position of large ice conglomerates in the ice sheet was determined by eye and was used as the lower boundary of the ice sheet at different times. The measured values of h as a function of time t are shown for both runs by points in Fig. 9. Typical error bars are also shown. The values of h, estimated using (30), with $I_0 = 0.25$ and u given by (6), are shown for comparison by dash lines for the two cases. In spite of significant simplifications, the model correctly predicts the behavior of h with time and gives realistic estimates.

Using the first points of the two runs, shown in Fig. 9, the mean initial nondimensional rate of ice formation $(dh/dt)/u$ was determined for both experiments and is shown in Fig. 10. The solid line indicates variation of $(dh/dt)/u$ with Ri_0, as estimated using (23) for $t = 0$. An interesting feature of this function is the presence of a maximum at moderate Ri_0 values ($\mathrm{Ri}_0 \approx 20$). However, it is impracticable to determine this maximum experimentally; at moderate Ri_0, the intensity of mixing across density interface becomes too high and the timescale τ_0, given by (28), becomes too small to expect frazil ice formation before the interface breaks up in small tank experiments. Figure 11 shows the interfacial structure at different Ri_0 values. Not the intense mixing at Ri ≈ 23, which may cause the layers to break up rapidly.

The existence of the maximum in Fig. 10 can be interpreted as a consequence of different rates of heat and salt transport across the density interface. At $t = 0$, (29) can be written in the form

$$\frac{dh/dt}{u} = \frac{c_p a}{\lambda I_0}\Delta S_0(c_t\,\mathrm{Ri}_0^{-1/2} - c_s\,\mathrm{Ri}_0^{-3/2}). \tag{31}$$

At large Ri_0 values, $\mathrm{Ri}_0 \gg c_s/c_t \approx 7$, the first term in the rhs of (31), which signifies the heat transport, dominates the second term that reckons the salt trans-

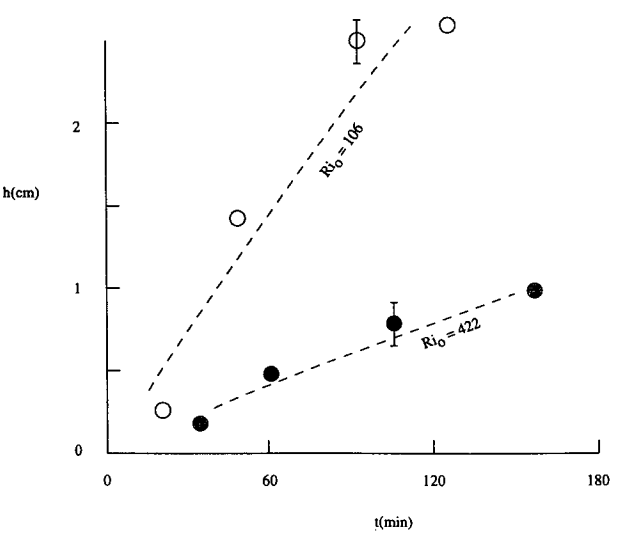

FIG. 9. Measured (open and solid dots) and calculated (dash lines) values of the ice-sheet thickness h as a function of time t for two experiments carried out at $\mathrm{Ri}_0 = 422$ (solid) and $\mathrm{Ri}_0 = 106$ (open). Typical error bars are also shown.

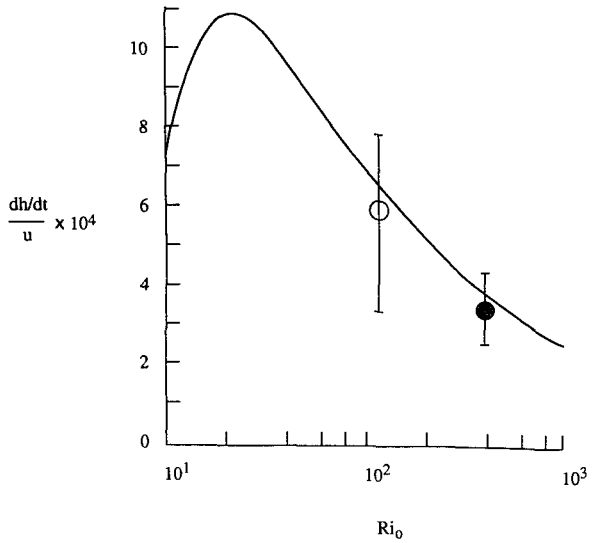

FIG. 10. The nondimensional rate $(dh/dt)/u$ of initial ice growth for different values of initial Richardson number Ri_0; dots are measured values, solid line is estimate based on (23) for $t = 0$. Large error bars reflect large scatter of data for the initial measurements of h.

port. As a result, the freezing temperature in the upper layer does not change significantly and practically all heat is used for the ice formation; in this limit, $(dh/dt)/u \sim \mathrm{Ri}_0^{1/2}$. When Ri_0 decreases, $(dh/dt)/u$ increases and reaches a maximum at moderate Ri_0 values ($\mathrm{Ri}_0 \approx 20$). At $\mathrm{Ri}_0 < 20$, the salt transport becomes significant, the freezing temperature decreases and part of the heat must be expended for cooling of more salty water; only the rest of the heat is now available for ice production. As a result, the function $(dh/dt)/u$ decreases with decreasing Ri_0. At small $\mathrm{Ri}_0 \to c_s/c_t \approx 7$, practically all heat must be spent on cooling of salty water and the freezing rate tends to be zero.

Finally, it is noted that although the condition (4) was realized in the experiments only approximately, the related condition $\Delta T + a\Delta S = 0$, which was essential in the model development, was realized with reasonable accuracy. Figure 12 shows the time variation of mean overcooling temperatures $T^0_{1,2} = T_{1,2} + aS_{1,2}$, for the upper ($T^0_1$) and lower ($T^0_2$) layers, estimated by the measured $S_{1,2}$ and $T_{1,2}$ for the experiment with $\mathrm{Ri}_0 = 106$. Although both layers were slightly overcooled during the experiment, the sum $\Delta T + a\Delta S = T^0_2 - T^0_1$ was nearly equal to zero.

5. Concluding remarks

In a system consisting of two shear-free turbulent layers of fresh and salt water at their respective freezing

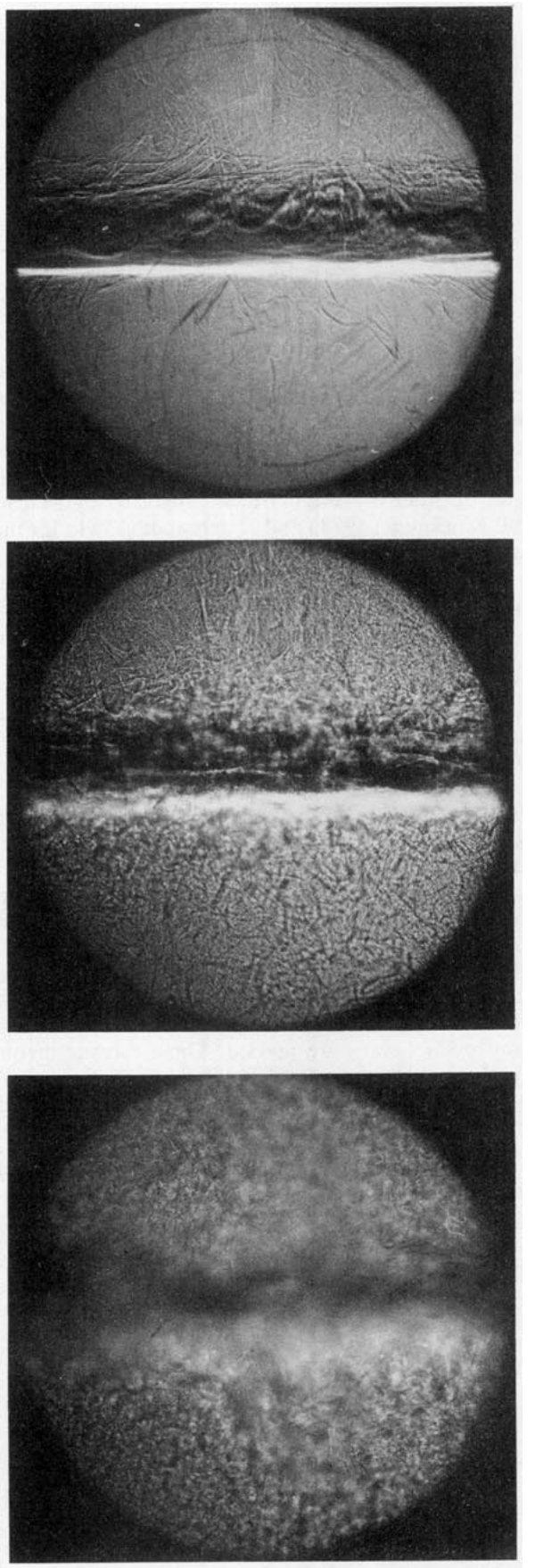

FIG. 11. Shadow graphs of the lighted circle of the density interface at $\mathrm{Ri}_0 = 422$ (upper), 94 (middle), and 23 (lower). The diameter is 17.5 cm.

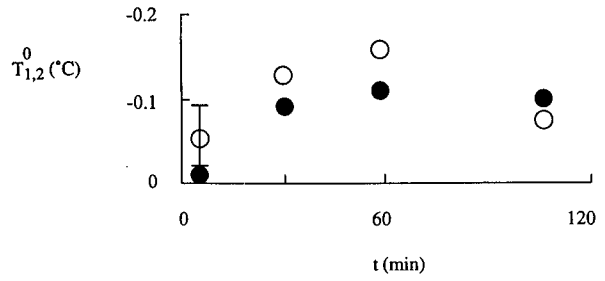

FIG. 12. Mean overcooling temperatures $T^0_{1,2} = T_{1,2} + aS_{1,2}$ for upper (open) and lower (solid) layers at different times; $Ri_0 = 106$.

points, the frazil ice can be formed and collected at the surface as a sheet of ice. The rate of growth of the ice sheet depends on the interfacial Richardson number and may reach from a few to many centimeters per day, that is, 30–100 times faster than the estimated rates of order 0.1–0.2 cm day^{-1} reported by Martin and Kauffman (1974) and Stigebrandt (1981) for the case when the turbulence is absent.

To extrapolate these results to natural situations one needs to have an idea of the local Richardson number and the nature of the background turbulence. Taking for the depth of fresh water $H_1 \approx 1$–2 m, which gives $l \approx 10$–20 cm, and for typical velocity scale of $u \approx 0.5$–1 cm s^{-1}, we obtain, for $\Delta S_0 = 35$ psu, the estimate $Ri_0 = 280$–2200. In accordance with the graph of Fig. 10, this gives an estimate for the rate of frazil ice formation in the presence of shear-free turbulence as $dh/dt = (1\text{–}4) \times 10^{-4}$ cm s^{-1} or (8–35) cm per day. This estimate, however, should be viewed with caution because of the multitude of phenomena that can be present in oceanic environments, which are not accounted for in the present work. In particular, shear-induced turbulence can be a major contributor in polar oceans, and the entrainment laws in the presence and absence of shear can be markedly different (Fernando 1991). To obtain more accurate estimates, additional field data from polar oceans are needed. These measurements should include the rate of frazil ice formation, temperature and salinity profiles, and the characteristics of turbulence.

Acknowledgments. This research was carried out during a visit of one of the authors (SIV) to the Environmental Fluid Dynamics Program at Arizona State University. The financial support for Geophysical Fluid Dynamics Research at ASU is provided by the Office of Naval Research (High Latitude Processes and Small-Scale Oceanography), National Science Foundation, and the Environmental Protection Agency. SIV is grateful to the Russian Basic Research Foundation for financial support. L. Mitchell was funded by an NSF Research Education for Undergraduates Award.

REFERENCES

Benilov, A. Y., S. I. Voropayev, and V. V. Zhmur, 1993: Modeling the evolution of the upper turbulent layers of the ocean during heating. *Bull (Izvestiya) Acad. Sci. USSR, Atmos. Oceanic Phys.*, **19,** 130–135.

Cherepanov, N. V., and A. M. Kozlovskii, 1972: The frazil ice of Antarctica coastal waters. *Inform. Bull. SAE,* **84,** 61–65.

E, X., and E. J. Hopfinger, 1986: On mixing across an interface in stably stratified fluid. *J. Fluid Mech.*, **166,** 227–244.

Fernando, H. J. S., 1991: Turbulent mixing in stratified fluids. *Ann. Rev. Fluid Mech.*, **23,** 455–475.

Hanson, A. N., 1965: Studies of the mass budget of Arctic pack-ice floes. *J. Glaciol.*, **5,** 701–709.

Hobbs, P. V. 1974: *Ice Physics.* Clarendon Press, 837 pp.

Hopfinger, E. J., and J. A. Toly, 1976: Spatially decaying turbulence and its relation to mixing across density interfaces. *J. Fluid Mech.*, **78,** 155–175.

Kantha, L. H., and R. R. Long, 1980: Turbulent mixing with stabilizing surface buoyancy flux. *Phys. of Fluids,* **23,** 2142–2143.

Kozlovskii, A. M., 1971: Frazil ice in the Gulf of Alasheev. *Trudy SAE,* **47,** 222–224.

Krylov, A. D., and A. G. Zatsepin, 1992: Frazil ice formation due to difference in heat and salt exchange across a density interface. *J. Mar. Sys.*, **3,** 497–506.

Lide, D. R., Ed., 1993: *CRC Handbook of Chemistry and Physics.* CRC Press.

Martin, S., 1981: Frazil ice in rivers and oceans. *Ann. Rev. Fluid Mech.*, **13,** 379–397.

——, and P. Kauffman, 1974: The evolution of under-ice melt pounds, or double diffusion at the freezing point. *J. Fluid Mech.*, **64,** 507–527.

Nansen, F., 1897: *Farthest North.* Harper & Brothers, 457–458.

Stigebrandt, A., 1981: On the rate of ice formation in water cooled by more saline sublayer. *Tellus,* **33,** 604–609.

Thompson, S. M., and J. S. Turner, 1975: Mixing across an interface due to turbulence generated by an oscillating grid. *J. Fluid Mech.*, **67,** 343–368.

Voropayev, S. I., A. G. Zatsepin, and A. D. Krylov, 1988: Coupled heat and salt transport across the density interface between turbulent layers. *Proc. Conf. Stratified Flows,* **2,** 133–136.

Zubov, N. N., 1963: *Arctic Ice.* U.S. Naval Oceanographic Office and Amer. Meteor. Soc. 491 pp. First published in Russian by Glasevmorput in 1945.